Received: 24 January 2022 | Revised: 27 June 2022 | Accepted: 21 July 2022

DOI: 10.1002/lio2.966

ORIGINAL RESEARCH

Laryngoscope Investigative Otolaryngology

CircBFAR correlates with poor prognosis and promotes laryngeal squamous cell cancer progression through miR-31-5p/COL5A1 axis

Hengcui Gong MM[1] | Wei Wu[2] | Chuankai Fang MM[3] | Di He MM[4]

[1]Department of Otolaryngology, Yibin Hospital of Traditional Chinese Medicine, Yibin, Sichuan, China

[2]Department of Radiotherapy, GanZhou Cancer Hospital/The Affiliated Cancer Hospital of Gannan Medical University, GanZhou, Jiangxi, China

[3]Department of Ophthalmology, Tongxiang First people's Hospital, Tongxiang, Zhejiang, China

[4]Department of Otorhinolaryngology, Tongxiang First people's Hospital, Tongxiang, Zhejiang, China

Correspondence
Di He, Department of Otorhinolaryngology, Tongxiang First people's Hospital, 25-2-101, Jinsejiayuan, Heping Rd, Zhendong New District, Tongxiang City 314500, Zhejiang Province, China.
Email: hedi411416@163.com

Abstract

Introduction: Laryngeal squamous cell cancer (LSCC) is a highly malignant tumor originating from the respiratory system. Circular RNAs have been reported to be associated with the treatment and prognosis of a variety of cancers, including LSCC.

Methods: The expression of circBFAR, miR-31-5p, and collagen type V alpha 1 chain (COL5A1) in LSCC tissues and cells was detected by quantitative real-time polymerase chain reaction. Cell counting kit 8 and 5-Ethynyl-2′-deoxyuridine assays were used to detect cell proliferation. Wound healing assay and transwell assay were used to test cell migration and invasion, respectively. The protein expression in LSCC cells was detected with western blot. The relationships between miR-31-5p and circBFAR or COL5A1 were identified by dual-luciferase reporter assay, RNA-pull down assay, and immunoprecipitation assay. The effect of circBFAR on tumor growth in vivo was detected by tumor xenograft mice experiment. The protein expression of COL5A1 and KI-67 in LSCC tissues was measured by immunohistochemistry assay.

Results: CircBFAR was increased in LSCC tissues and cells, and was related to advanced clinical stage and overall survival of LSCC patients. The cell viability and proliferation were inhibited by circBFAR knockdown and silencing of circBFAR blocked migration and invasion of LSCC cells. CircBFAR knockdown suppressed cell tube formation, and the protein expression of KI-67, matrix metallopeptidase 2 (MMP2), and vascular endothelial growth factor A (VEGFA) in LSCC cells. MiR-31-5p was the target of circBFAR, and the inhibitory effects of circBFAR deficiency on viability, proliferation, migration, invasion, tube formation and the protein expression of KI-67, MMP2, and VEGFA in LSCC cells were rescued by miR-31-5p downregulation. COL5A1 was negatively regulated by miR-31-5p, and was boosted in LSCC tissues and cells. COL5A1 overexpression reversed the inhibitory effects of miR-31-5p on LSCC cells. CircBFAR insufficiency hindered tumor growth in vivo.

Conclusion: CircBFAR, miR-31-5p, and COL5A1 in LSCC progression might provide novel therapeutic targets for LSCC clinical intervention.

Hengcui Gong and Wei Wu contribute to this work equally as co-first authors.

KEYWORDS
CircBFAR, COL5A1, laryngeal squamous cell cancer, miR-31-5p

1 | INTRODUCTION

Laryngeal squamous cell cancer (LSCC) is a malignant tumor occurring in the larynx and is the most common pathological type of laryngeal cancer.[1] With the progress of medical technology including surgery, chemotherapy, radiotherapy, and immunotherapy, the treatment of LSCC has made important progress, but the prognosis of patients is still poor.[2] Therefore, it is very important to understand the pathogenesis of LSCC and find molecular targets for the treatment of LSCC.

In recent years, circular RNAs (circRNAs) represent a class of endogenous non-coding RNAs, which are often formed by noncanonical back-splicing events.[3] Most of them have a covalently closed single-stranded circular structure that is not affected by exonucleases and is not easily degraded.[4] Furthermore, owing to the high stability, abundance, and evolutionary conservation, circRNAs have unique advantages as biomarkers of various human cancers,[5,6] containing LSCC.[7] For example, down-regulation of circ_0057481 functioned as a sponge of miR-200C to inhibit the growth, cell cycle progression, invasion, and migration potential of laryngeal carcinoma cells and promoted apoptosis.[8] Circ_0000218 was up-regulated in LSCC cells and negatively regulated the expression of miR-139-3p to promote LSCC cell viability and inhibit apoptosis.[9] Of note, previous studies suggested that circBFAR frequently acted as a carcinogenic factor by regulating cell proliferation, invasion, and glycolysis in diverse tumors.[10,11] However, the role and mechanism of circBFAR in the development of LSCC have not been reported.

MiRNAs are a class of noncoding RNAs that are not directly involved in protein expression and take part in the progress of LSCC,[12] such as miR-196b and miR-195.[13,14] It has been reported that miR-31-5p inhibited breast cancer cell proliferation and promoted apoptosis.[15] Interestingly, miR-31-5p was a form of mature miR-31, which has been previously validated to suppress LSCC cell growth and invasion in vitro.[16] Therefore, we further explored whether the regulatory role of circBFAR on LSCC development is mediated by miR-31-5p.

MiRNAs and mRNAs were enriched in a network and differentially expressed in LSCC.[17] Collagen type V alpha 1 chain (COL5A1) has been reported to be related to clear cell renal cell carcinoma,[18] lung adenocarcinoma,[19] breast cancer,[20] and so forth. COL5A1 was notably elevated in GC as an oncogene and was positively correlated with immune infiltration.[21] COL5A1 was greatly enhanced in ovarian cancer cells and tissues, which was positively correlated with proliferation, migration, and drug resistance of ovarian cancer cells.[22] But, the role of COLA51 in LSCC has not been studied, and the contact of circBFAR, COL5A1, and miR-31-5p has not been reported.

Nowadays, increasing attention has been paid to the regulatory mechanism of the circRNAs–miRNAs–mRNAs in disease research.[23] It has been confirmed that circRNAs might function as competing endogenous RNAs to sequester miRNAs away from target mRNAs.[24] In this study, we concentrated on the function and mechanism of circBFAR in LSCC. The regulation of circBFAR through miR-31-5p and COL5A1 in the development of LSCC was explored for the first time, and the diagnostic value of circBFAR/miR-31-5p/COL5A1 axis in LSCC patients was confirmed.

2 | MATERIALS AND METHODS

2.1 | Clinical tissue samples

This experiment was recognized by the Ethics Committee of Yibin Hospital of Traditional Chinese Medicine. LSCC tissues and normal tissues of 68 LSCC patients from Yibin Hospital of Traditional Chinese Medicine were collected, and all patients voluntarily signed written informed consent. Meanwhile, morphologically normal mucosa tissues that were more than 5 cm from the cancerous tissues were used as adjacent noncancerous tissues. Based on the median value of circBFAR level, 68 LSCC patients were zoned as high expression group of circBFAR and low expression group of circBFAR. Once in isolation, these clinical organizations were refrigerated in liquid nitrogen offhand and reserved in a − 80°C refrigerator. The detailed clinical characteristics of patients are described in Table 1.

2.2 | Cell lines

Cell Bank of the Chinese Academy of Sciences (Shanghai, China) furnished the LSCC cell lines (TU177, M4E, AMC-HN-8, and TU686) and normal nasopharyngeal cell line (NP69). All cells were contained in Dulbecco's modified Eagle's medium (Gibco, Rockville, Maryland) which contains 10% fetal bovine serum (FBS; Biological Industries, Kibbutz Beit Haemek, Israel) with a 37°C cell incubator (Panasonic, Osaka, Japan) contained 5% CO_2.

2.3 | Quantitative real-time polymerase chain reaction

The RNA in LSCC tissues and cells was acquired with the Trizol Reagent (TIANGEN, Beijing, China), and cDNA was compounded with AMV Reverse Transcriptase (Solarbio) and quantified by SYBR Green Realtime PCR Master Mix (Toyobo Co., Osaka, Japan). Glyceraldehyde 3-phosphate dehydrogenase (GAPDH) and small nuclear RNA (U6) were chosen as the internal steward genes, and relative RNA expression was calculated by the $2^{-\Delta\Delta Ct}$ method. BGI (Beijing, China)

TABLE 1 Correlation between circBFAR expression and clinical feature in LSCC patients

Clinical feature	*n*	circBFAR		*p*-value
		High	Low	
Age (years)				.139
≥60	40	23	17	
<60	28	11	17	
Smoking status				.625
Nonsmoker	30	14	16	
Smoker	38	20	18	
T stage				.143
T1/T2	30	12	18	
T3/T4	38	22	16	
Clinical stage				.029*
I/II	35	13	22	
III/IV	33	21	12	
Lymph node metastasis				.015*
Negative	32	11	21	
Positive	36	23	13	

Abbreviations: LSCC, laryngeal squamous cell cancer.
*p < .05.

was hired to synthesize primers, and the primer sequences were shown as follows:

circBFAR: 5′-CCAAACCTCAAGAATGCAGGC-3′ (sense), 5′-CCCTGCTTCAGCAGTATCCA-3′ (antisense);
COL5A1: 5′-CTTGGCCCAAAGAAAACCCG-3′ (sense), 5′-GCGTCCACATAGGAGAGCAG-3′ (antisense);
SPARC: 5′-CATTGCACCACCCGCTTTTT-3′ (sense), 5′-GATATCCTTCTGCTTGATGCCG-3′ (antisense);
miR-31-5p: 5′-GTATGATCTTGGAGTAGGTCA-3′ (sense), 5′-CTCAACTGGTGTCGTGGAG-3′ (antisense);
U6: 5′-CTCGCTTCGGCAGCACA-3′ (sense), 5′-AACGCTTCACGAATTTGCGT-3′ (antisense);
GAPDH: 5′-GACAGTCAGCCGCATCTTCT-3′ (sense), 5′-GCGCCCAATACGACCAAATC-3′ (antisense).

2.4 | Cell transfection

Transfection plasmids: short hairpin-circBFAR (sh-circBFAR), miR-31-5p mimic/inhibitor (miR-31-5p/anti-miR-31-5p), pcDNA-COL5A1 (COL5A1), and their negative controls (sh-NC, miR-NC, anti-NC, and vector) were gained from Nanjing Kebai Biological Technology Co., Ltd (Nanjing, China). When the confluence of TU177 and AMC-HN-8 cells reached 70–80%, the plasmids were transfected into these cells using Lipofectamine 2000 reagent (Invitrogen, Carlsbad, California). At 48 h after transfection, quantitative real-time polymerase chain reaction (qRT-PCR) was employed to test the transfection efficiency.

2.5 | Cell counting kit 8 assay

A total of 100 μl TU177 and AMC-HN-8 cells were added to the 6-well plate, respectively. After transfection and cultured for a period of time, the cells were hatched with 10 μl cell counting kit 8 (CCK8) solution (Shanghai Enzyme-linked Biotechnology Co., Ltd., Shanghai, China) for 1 h. The absorbance at 450 nm was measured every 24 h.

2.6 | 5-Ethynyl-2′-deoxyuridine assay

5-Ethynyl-2′-deoxyuridine (EdU) assay was employed to detect the ability of cell proliferation with the EdU Staining Proliferation Kit (Abcam, Cambridge, England). In brief, the cells to be detected were stained with EdU solution for 2–4 h and incubated with 4% paraformaldehyde (Sigma-Aldrich, St. Louis, Missouri) for 15 min. After being incubated with Apollo Dye Solution for 30 min, the cells were stained with 4′,6-diamidino-2-phenylindole (DAPI) for 30 min, followed by a photograph with a fluorescence microscope (Olympus, Tokyo, Japan) for analysis.

2.7 | Wound healing assay

A total of 70 μl cells with a density of 3×10^5 cells/ml were appended to the ibidi petri dish (ibidi GmbH, Martin Reid, Germany). The healing plug was removed 24 h later, and fresh medium was added. Initial scratch images and scratch images after 24 h were taken under the microscope (Olympus).

2.8 | Transwell assay

.The ability of cell invasion was monitored with the transwell chambers (Coster, Perot, Italy) containing matrigel (BD, Franklin Lakes, New Jersey). The lower compartment of the 24-well plate was added with a 500 μl medium which has 10% FBS. The Transwell compartment was placed into the 24-well plate, and 100 μl cell suspension was cultured for 24 h in the upper compartment. The chamber was removed and the medium was abandoned. Matrigel and the cells in the upper chamber were swabbed gently. And the chamber was fixed with 600 μl 4% paraformaldehyde (Sigma-Aldrich) in a new 24-well plate for 20–30 min, then the fixative was discarded, and the cells were dyed with 0.1% crystal violet for 5–10 min, washed tardily with phosphate buffer saline (Biological Industries) for three times, and observed with the high-power microscope and took pictures. Then, migration cells were counted in five random fields of view, and the mean ± SD was calculated accordingly.

2.9 | Angiogenesis assay

A total of 100 μl matrix gel (BD) was added to a 96-well culture plate and polymerized at 37°C for 30 min. Cells with a density of 4×10^5

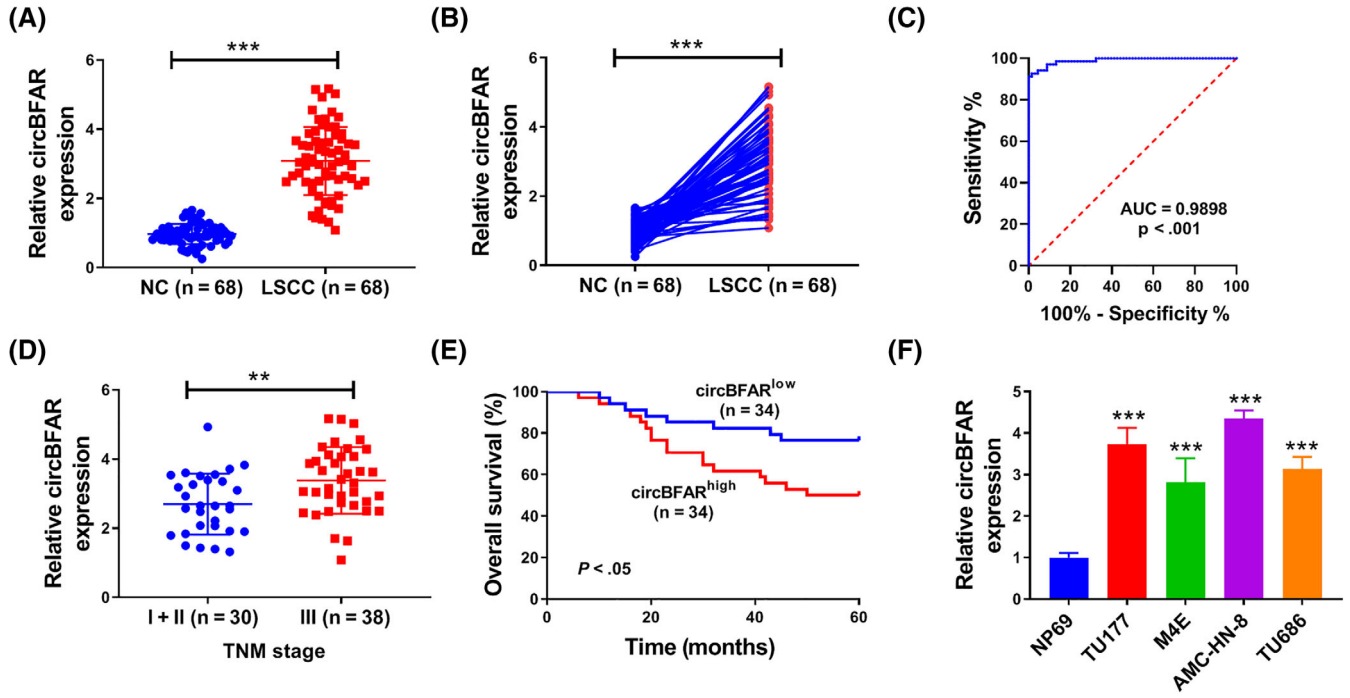

FIGURE 1 The expression of circBFAR was increased in laryngeal squamous cell cancer (LSCC) tissues and cells. (A,B) The expression level of circBFAR in LSCC tumor tissues ($n = 68$) and normal tissues ($n = 68$) was detected by quantitative real-time polymerase chain reaction (qRT-PCR). (C) Receiver operating characteristic curve analysis of circBFAR for diagnostic potentiality in LSCC. (D) Relationship between circBFAR expression level and clinical stages in LSCC patients. (E) The overall survival rate in LSCC patients with high circBFAR expression ($n = 34$) and patients with low circBFAR expression ($n = 34$) was evaluated using Kaplan–Meier overall survival curve. (F) The expression level of circBFAR in normal cell line NP69 and LSCC cell lines (TU177, M4E, AMC-HN-8, and TU686) was detected using qRT-PCR assay. *$p < .05$. All cellular experiments were independently repeated three times, and the data were presented in the format of mean ± SD. AUC, area under the curve; NC, negative controls

cells/ml were added to the matrix coating well. After 24 h cultured at 37°C, the tube formation was measured by microscope (Olympus).

2.10 | Western blot

A protein extraction kit (Beyotime Biotechnology, Jiangsu, China) and BCA Protein Assay Kit (Beyotime Biotechnology) were employed to extract and quantify protein in TU177 and AMC-HN-8 cells, respectively. SDS-PAGE Kit (Shanghai Guduo Biological Technology Co., Ltd, Shanghai, China) was used for protein separation. The protein was transferred into the polyvinylidene fluoride (PVDF) membrane (Millipore, Billerica, Massachusetts). PVDF membrane was closed with 5% bovine serum albumin (Saibao Biotechnology Co., Ltd., Jiangsu, China), and then was hatched with the primary antibodies (anti-KI-67 antibody, 1:5000, ab92742; antimatrix metallopeptidase 2 (MMP2) antibody, 1:1000, ab92536 and antivascular endothelial growth factor A (VEGFA) antibody, 1:10 000, ab52917; anti-beta actin (β-actin) antibody, 1:1000, ab8227; Abcam) and secondary antibodies (1:2000, ab6721, Abcam), respectively. Immobilon Western Chemiluminescent HRP Substrate (Merck, Darmstadt, Hesse, Germany) was dropped onto the PVDF membrane, and the bands were photographed in a gel imaging analyzer (UVITEC, Cambridge, England).

2.11 | Dual-luciferase reporter assay

Firstly, the sequences containing the predicated miR-31-5p binding sites of circBFAR and COL5A1 were obtained by PCR and then introduced into psiCHECK-2vector (Promega, Madison, Wisconsin), generating circBFAR-WT and COL5A1-3′untranslated region (UTR)-WT. The mutant constructs (circBFAR-MUT and COL5A1-3′UTR- MUT) were obtained by a QuikChange II site-directed Mutagenesis kit (Agilent Technologies, Inc., Santa Clara, California). The TU177 and AMC-HN-8 cells were transfected with circBFAR-WT, circBFAR-MUT, COL5A1-3′UTR-WT, and COL5A1-3′UTR-MUT and miR-31-5p mimics (miR-31-5p) or miR-NC, respectively. After being transfected for 48 h, Dual-Luciferase Reporter Gene Assay Kit (Yeasen Biotechnology, Shanghai, China) was employed to detect the luciferase activity in every group.

2.12 | RNA-pull down assay

Bio-labeled circBFAR (Bio-circBFAR) or its negative control (Bio-NC; Sangon Biotech, Shanghai, China) were hatched with lysate cells. Then the complex was bound to the magnetic beads, and the RNA content in the complex was segregated and detected by qRT-PCR.

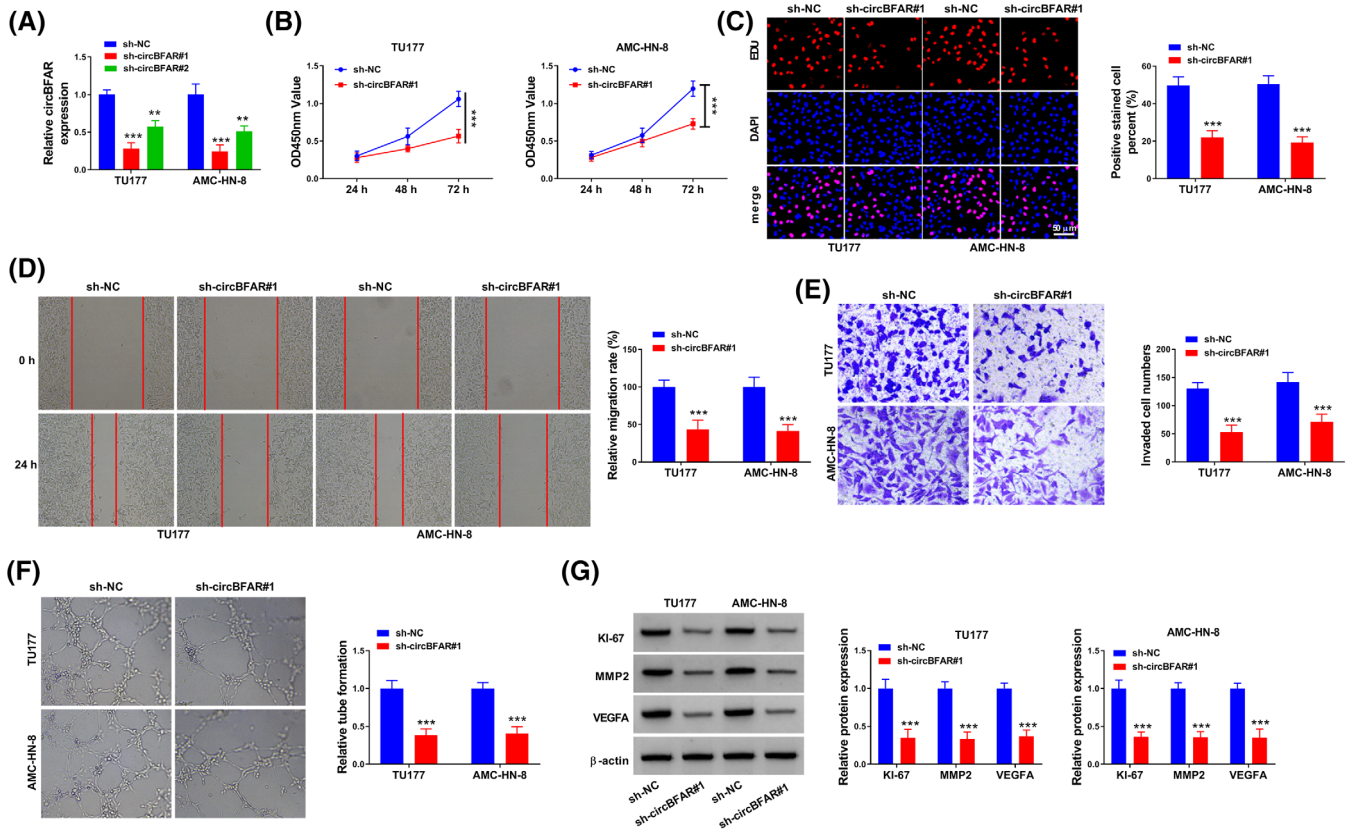

FIGURE 2 CircBFAR knockdown suppressed cell proliferation and angiogenesis in laryngeal squamous cell cancer (LSCC) cells. (A) quantitative real-time polymerase chain reaction was performed to detect the efficiency of sh-circBFAR#1 and sh-circBFAR#2 in TU177 and AMC-HN-8 cells. (B) Cell counting kit 8 assay was used to test cell viability of TU177 and AMC-HN-8 cells after sh-circBFAR#1 transfection. (C) 5-Ethynyl-2′-deoxyuridine assay was conducted to evaluate the effect of sh-circBFAR#1 on cell proliferation. (D) The ability of transfected cells to migrate was detected by the wound healing assay. (E) The effect of sh-circBFAR#1 on cell invasion was tested by transwell assay. (F) Effects of sh-circBFAR#1 on tube formation in TU177 and AMC-HN-8 cells were measured using tube formation assay. (G) Effects of sh-circBFAR#1 on protein expression of KI-67, MMP2, and VEGFA in TU177 and AMC-HN-8 cells were assessed using western blot assay (*$p < .05$). All cellular experiments were independently repeated three times, and the data were presented in the format of mean ± SD. MMP2, matrix metallopeptidase 2; vascular endothelial growth factor A

2.13 | RNA immunoprecipitation assay

A total of 100 μl TU177 and AMC-HN-8 cells were split with RNA immunoprecipitation (RIP) lysis buffer and cultured in RIP buffer which containing magnetic beads coupled with anti-Ago2 (Abcam) or anti-immunoglobin G (IgG) (Abcam). After co-culture with protease K, the content of circBFAR and miR-31-5p in the precipitate was detected by qRT-PCR.

2.14 | Immunohistochemistry assay

Tumor tissue was fixed with paraformaldehyde (Sigma-Aldrich) and embedded with paraffin (Sangon Biotech), followed by cutting into 4 μm sections. The slices were treated with diluted COL5A1 (1:100, ab189285; Abcam) and KI-67 antibody (1:100, ab15580; Abcam) and the secondary antibody (1:1000, ab150077; Abcam), respectively. The samples were dyed with diaminobenzidine (Sigma-Aldrich) and observed under a microscope (Olympus).

2.15 | Tumor xenograft mice model construction

A total of 12 nude mice from Vital River Laboratory Animal Technology (Beijing, China) were randomly divided into two groups, with 6 mice in each group. In total, 3×10^6 AMC-HN-8 cell suspension was blown evenly and subcutaneously injected into mice. The size of the tumor was measured every 7 days, according to the formula: volume = length × width^2/2. The mice were slain painlessly after 35 days, and the mass of the tumor was weighed. The Animal Welfare and Research Ethics Committee of Yibin Hospital of Traditional Chinese Medicine agreed with all animal experiments in this study.

2.16 | Statistical analysis

SPSS 17.0 (IBM, Chicago, Illinois) was engaged to analyze the data, and images were made with GraphPad Prism 8.0 software (GraphPad Inc., LaJolla, California). Data were manifested as mean ± SD.

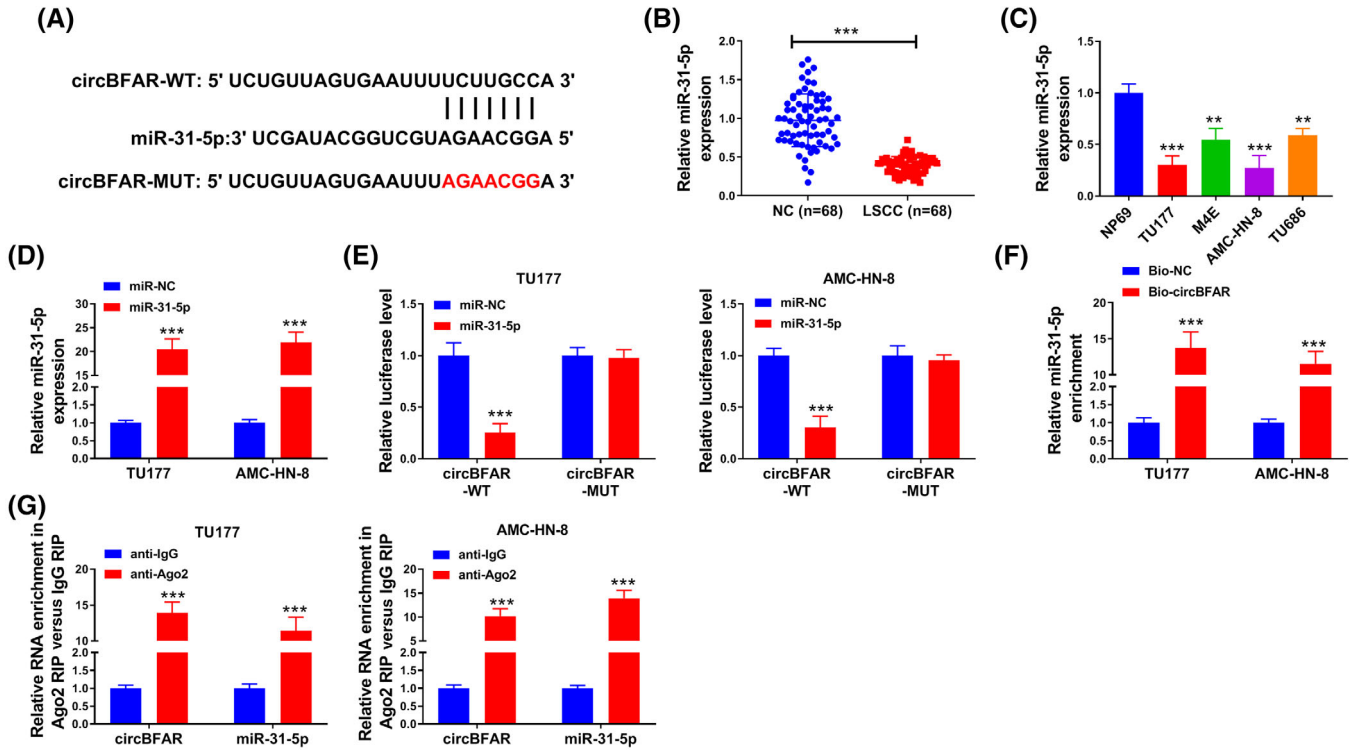

FIGURE 3 MiR-31-5p was a target of circBFAR. (A) The binding sequence between circBFAR and miR-31-5p was predicted by circinteractome. (B,C) Quantitative real-time polymerase chain reaction (qRT-PCR) was performed to detect the expression of miR-31-5p in laryngeal squamous cell cancer tissues and cells. (D) The transfection efficiency of miR-31-5p mimics in TU177 and AMC-HN-8 cells was examined using qRT-PCR assay. (E) Dual-luciferase reporting assay was performed to verify the targeting relationship between circBFAR and miR-31-5p in TU177 and AMC-HN-8 cells. (F) RNA-pull down assay was employed to analyze the interaction between circBFAR and miR-31-5p. (G) RNA immunoprecipitation assay was conducted for the enrichment of Ago2 on miR-31-5p and circBFAR in TU177 and AMC-HN-8 cells (*p < .05). All cellular experiments were independently repeated three times, and the data were presented in the format of mean ± SD.
NC, negative controls

Kaplan–Meier survival analysis and log-rank test were applied to analyze the overall survival of LSCC patients. The diversities of data were tested with a one-way analysis of variance or Student's t-test. A p-value < .05 indicated significant difference between data. The receiver operating characteristic (ROC) curve analysis was conducted to assess the area under the curve (AUC) values for circBFAR in LSCC samples.

3 | RESULTS

3.1 | CircBFAR was highly expressed in LSCC tissues and cells

In order to explore the function and regulatory mechanism of circBFAR in the progression of LSCC, we first detected the expression of circBFAR in LSCC. The results showed that circBFAR was significantly promoted in LSCC tissues (Figure 1A,B). Then the sensitivity and specificity were evaluated by ROC curve analysis, and the results of ROC exhibited that the AUC of circBFAR was 0.9898 (Figure 1C). And the high expression of circBFAR was related to the advanced clinical stage in LSCC patients (Figure 1D). The overall survival of the low circBFAR expression group (n = 34) was higher than the high expression group (n = 34) in LSCC patients (Figure 1E). Meanwhile, our data showed that circBFAR expression was associated with clinical stage and lymph node metastasis (Table 1). Moreover, we also discovered that circBFAR expression was significantly upregulated in LSCC cell lines relative to NP69 cells (Figure 1F). These data indicated that circBFAR was increased in LSCC cells and patients, and high expression of circBFAR might be an independent prognostic factor for the prediction of clinical outcomes in LSCC sufferers.

3.2 | Knockdown circBFAR inhibited the proliferation, migration, and invasion of LSCC cells and angiogenesis

In vitro function experiments were performed to detect the role of circBFAR in LSCC cells. QRT-PCR was used to detect the transfection efficiency of circBFAR in TU177 and AMC-HN-8 cells, and the results showed that the expression of circBFAR was dramatically inhibited in TU177 and AMC-HN-8 cells after sh-circBFAR#1 or sh-circBFAR#2 transfection, and sh-circBFAR#1 showed the best transfection

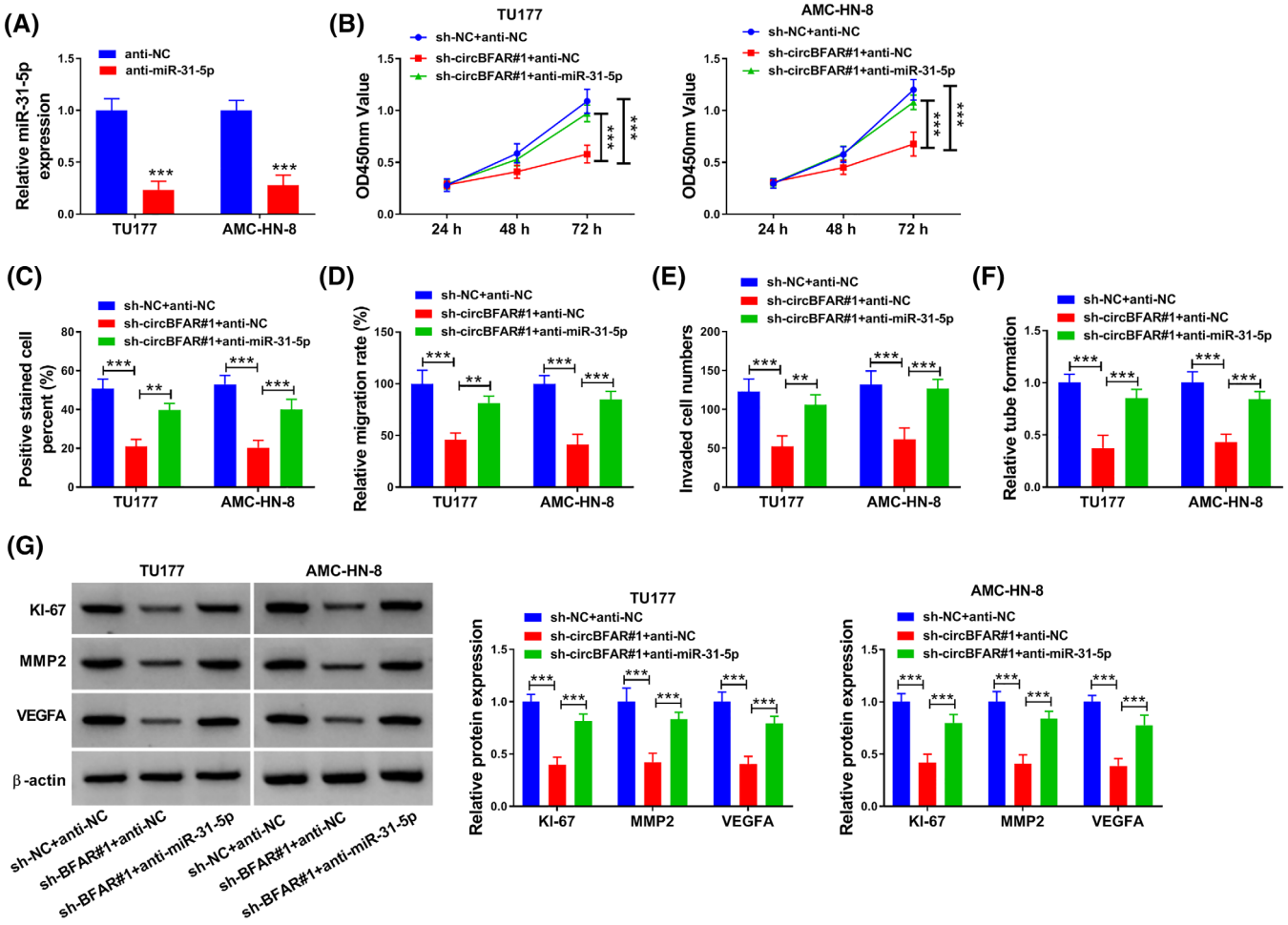

FIGURE 4 Anti-miR-31-5p reversed the effects of sh-circBFAR#1 on TU177 and AMC-HN-8 cells. (A) The expression of miR-31-5p was measured by qRT-PCR after transfection with anti-NC and anti-miR-31-5p in TU177 and AMC-HN-8 cells. (B–F) The effects of cell viability, proliferation, migration, invasion, and tube formation after transfection with sh-NC + anti-NC, sh-circBFAR#1 + anti-NC, and sh-circBFAR#1 + anti-miR-31-5p in TU177 and AMC-HN-8 cells. (G) Effects of sh-NC + anti-NC, sh-circBFAR#1 + anti-NC, or sh-circBFAR#1 + anti-miR-31-5p on protein expression of KI-67, MMP2, and VEGFA in TU177 and AMC-HN-8 cells were analyzed using western blot assay (*$p < .05$). All cellular experiments were independently repeated three times, and the data were presented in the format of mean ± SD. MMP2, matrix metallopeptidase 2; NC, negative controls; VEGFA, vascular endothelial growth factor A

efficiency (Figure 2A). CCK8 assay was performed to assess the cell viability, and the results exhibited that the cell viability of TU177 and AMC-HN-8 cells was reduced by sh-circBFAR#1 (Figure 2B). EdU assay exhibited that the proliferation was markedly retarded in TU177 and AMC-HN-8 cells transfected with sh-circBFAR#1 (Figure 2C). Wound healing results displayed that sh-circBFAR#1 repressed cell migration of TU177 and AMC-HN-8 cells (Figure 2D). And the ability of invasion in TU177 and AMC-HN-8 cells was tested by transwell, and the data showed that the invasion was reduced by sh-circBFAR#1 (Figure 2E). After TU177 and AMC-HN-8 cells were transfected with sh-circBFAR#1, the tube formation was remarkably retarded (Figure 2F). And circBFAR knockdown in TU177 and AMC-HN-8 cells exceptionally blocked the marker protein expression of KI-67, MMP2 and VEGFA (Figure 2G). In a word, the silence of circBFAR in LSCC cells inhibited cell growth and angiogenesis.

3.3 | CircBFAR targeted miR-31-5p in LSCC cells

For the purpose of probing the regulatory mechanism of circBFAR in LSCC, we first predicted the target of circBFAR with circinteractome (https://circinteractome.nia.nih.gov), and the binding sites between miR-31-5p and circBFAR were shown in Figure 3A. And we found the expression of miR-31-5p was striking hindered in LSCC tissues and cells (Figure 3B,C). Then the transfection efficiency of miR-31-5p was detected, and miR-31-5p was conspicuously boosted in TU177 and AMC-HN-8 cells with miR-31-5p overexpression (Figure 3D). The data of the dual-luciferase reporting assay presented that the luciferase activity in miR-31-5p and circBFAR cotransfection group was notably confined (Figure 3E). And RNA-pull down assay and RIP assay also proved the targeting relationship between circBFAR and miR-31-5p (Figure 3F,G). In sum, these data exhibited that miR-31–3p was regulated by circBFAR in LSCC cells.

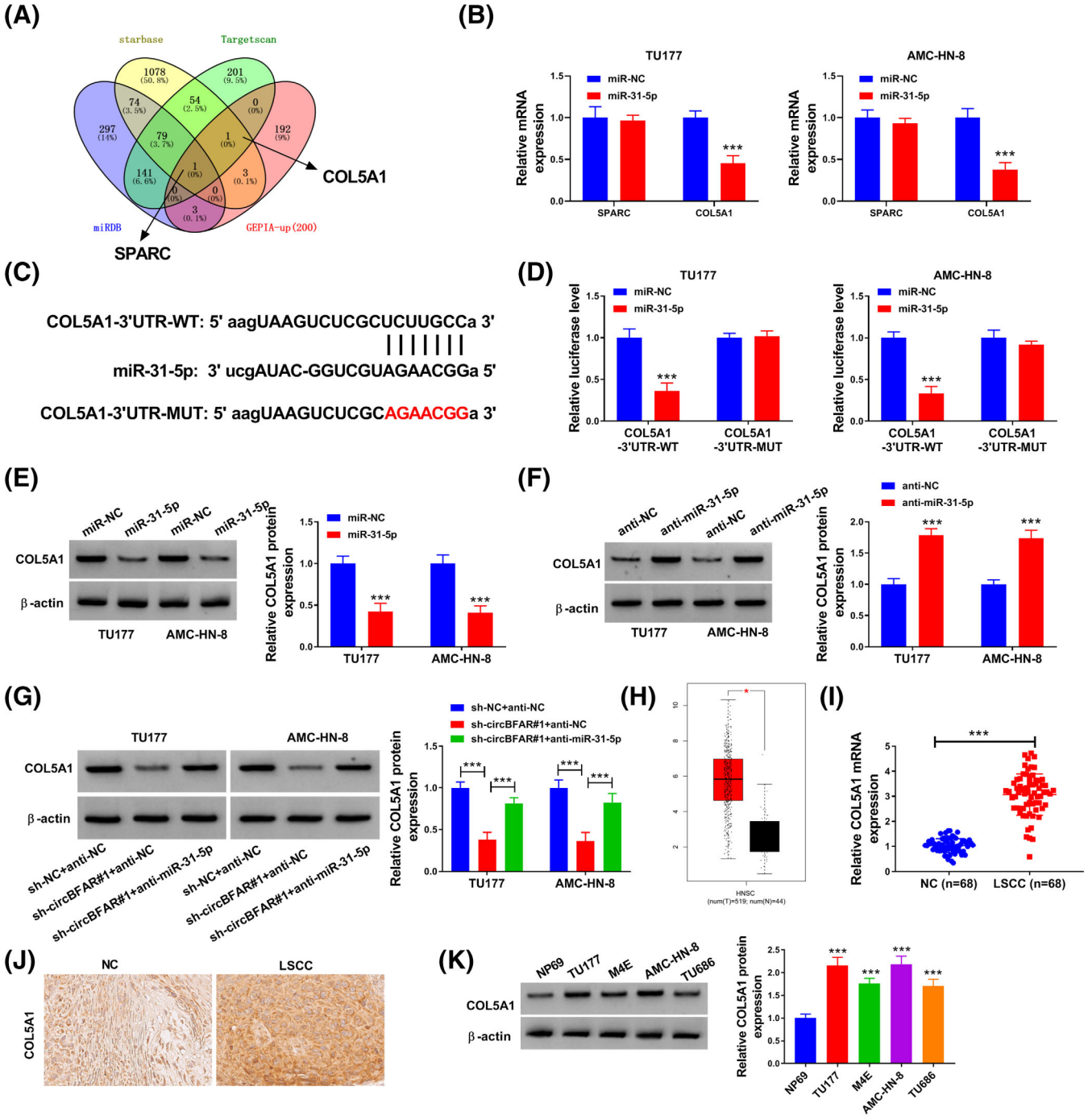

FIGURE 5 Collagen type V alpha 1 chain (COL5A1) was negatively regulated by miR-31-5p. (A) Targets of miR-31-5p were analyzed by starbase, Targetscan, miRDB, and GEPIA-up (200). (B) The expression levels of SPARC and COL5A1 in TU177 and AMC-HN-8 cells after miR-31-5p overexpression were detected using quantitative real-time polymerase chain reaction (qRT-PCR) assay. (C) The binding sites between COL5A1 and miR-31-5p were predicted. (D) Dual-luciferase reporting assay was performed to verify the targeting relationship between miR-31-5p and COL5A1 in TU177 and AMC-HN-8 cells. (E) The expression of COL5A1 in TU177 and AMC-HN-8 cells after miR-31-5p overexpression was detected by western blot. (F) The expression of COL5A1 protein in TU177 and AMC-HN-8 cells after anti-miR-31-5p transfection was determined using a western blot assay. (G) The expression of COL5A1 in TU177 and AMC-HN-8 cells after sh-NC + anti-NC, sh-circBFAR#1 + anti-NC or sh-circBFAR#1 + anti-miR-31-5p was transfected was measured using western blot assay. (H) The expression of COL5A1 in the head and neck squamous cell carcinoma of the TCGA database was analyzed. (I–K) The expression of COL5A1 in LSCC tissues and cells was tested using qRT-PCR, immunohistochemistry, and western blot assay (*p < .05). All cellular experiments were independently repeated three times, and the data were presented in the format of mean ± SD. LSCC, laryngeal squamous cell cancer; NC, negative controls

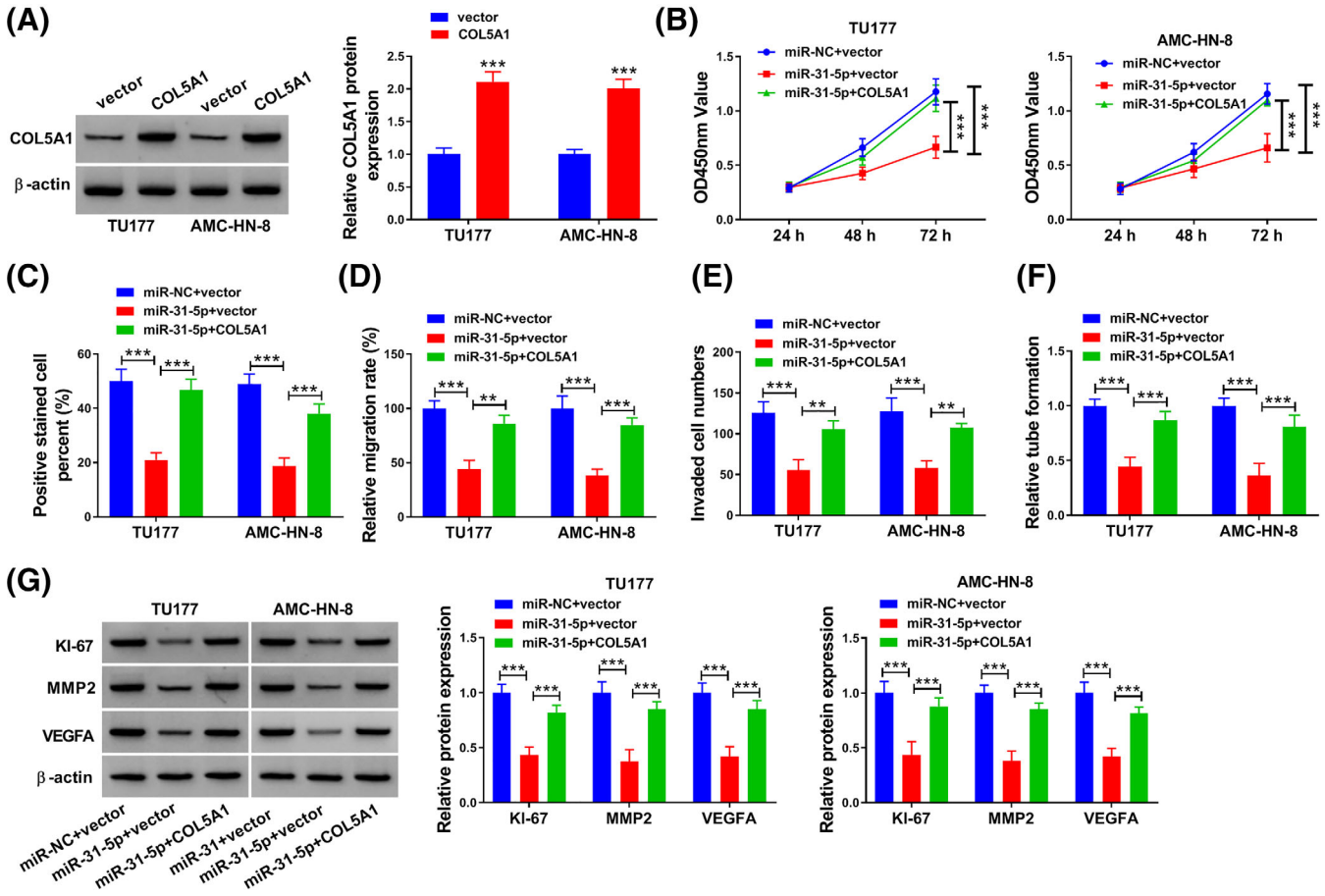

FIGURE 6 Collagen type V alpha 1 chain (COL5A1) overexpression reversed the effects of miR-31-5p in TU177 and AMC-HN-8 cells. (A) The expression of COL5A1 was measured after transfection with vector or COL5A1 in TU177 and AMC-HN-8 cells. (B to G) The effects of miR-31-5p on cell viability, proliferation, migration, invasion, tube formation, and the protein expression of KI-67, matrix metallopeptidase 2 (MMP2), and vascular endothelial growth factor A (VEGFA) after transfection with miR-NC + vector, miR-31-5p + vector or miR-31-5p + COL5A1 in TU177 and AMC-HN-8 cells were analyzed using cell counting kit 8 assay, 5-ethynyl-2′-deoxyuridine assay, wound healing assay, transwell assay, tube formation assay, and western blot assay (*p < .05). All cellular experiments were independently repeated three times, and the data were presented in the format of mean ± SD

3.4 | miR-31-5p knockdown could partially reverse the effects of sh-circBFAR#1 on LSCC cells

The inhibition efficiencies of anti-miR-31-5p in TU177 and AMC-HN-8 cells were first detected, and the results showed that anti-miR-31-5p had a better inhibition effect (Figure 4A). Sh-circBFAR#1 repressed cell viability of TU177 and AMC-HN-8 cells, while anti-miR-31-5p cotransfection reversed this effect (Figure 4B). And we confirmed that the inhibitory effect of sh-circBFAR#1 on proliferation was abolished by anti-miR-31-5p introduction (Figure 4C). And miR-31-5p knockdown partially overturned the suppressive impacts of circBFAR downregulation on migration and invasion in TU177 and AMC-HN-8 cells (Figure 4D,E). Silence of circBFAR limited the tube formation in TU177 and AMC-HN-8 cells, while this effect was abrogated after miR-31-5p knockdown (Figure 4F). We also found that anti-miR-31-5p relieved the inhibitory effects of sh-circBFAR#1 on the protein expression of KI-67, MMP2, and VEGFA in TU177 and AMC-HN-8 cells (Figure 4G). In summary, the inhibitory effects of sh-circBFAR#1 on LSCC cells were restored after anti-miR-31-5p was cotransfected.

3.5 | COL5A1 was a target of miR-31-5p in LSCC cells

The binding between miR-31-5p and COL5A1 or SPARC was predicted though starbase (https://starbase.sysu.edu.cn/), Targetscan (http://www.targetsc.an.org/vert_72/), miRDB (http://www.mirdb.org/), and GEPIA-up (200, http://gepia.cancer-pku.cn/index.html) (Figure 5A). Subsequently, we detected the changes in the expression levels of SPARC and COL5A1 after the overexpression of miR-31-5p in TU177 and AMC-HN-8 cells and found that the expression of SPARC did not change, while the expression of COL5A1 was greatly decreased, indicated that COL5A1 might be the target of miR-31-5p (Figure 5B). And the binding sites between miR-31-5p and COL5A1 were shown in Figure 5C. The luciferase activity was substantially repressed in COL5A1-3′UTR-WT and

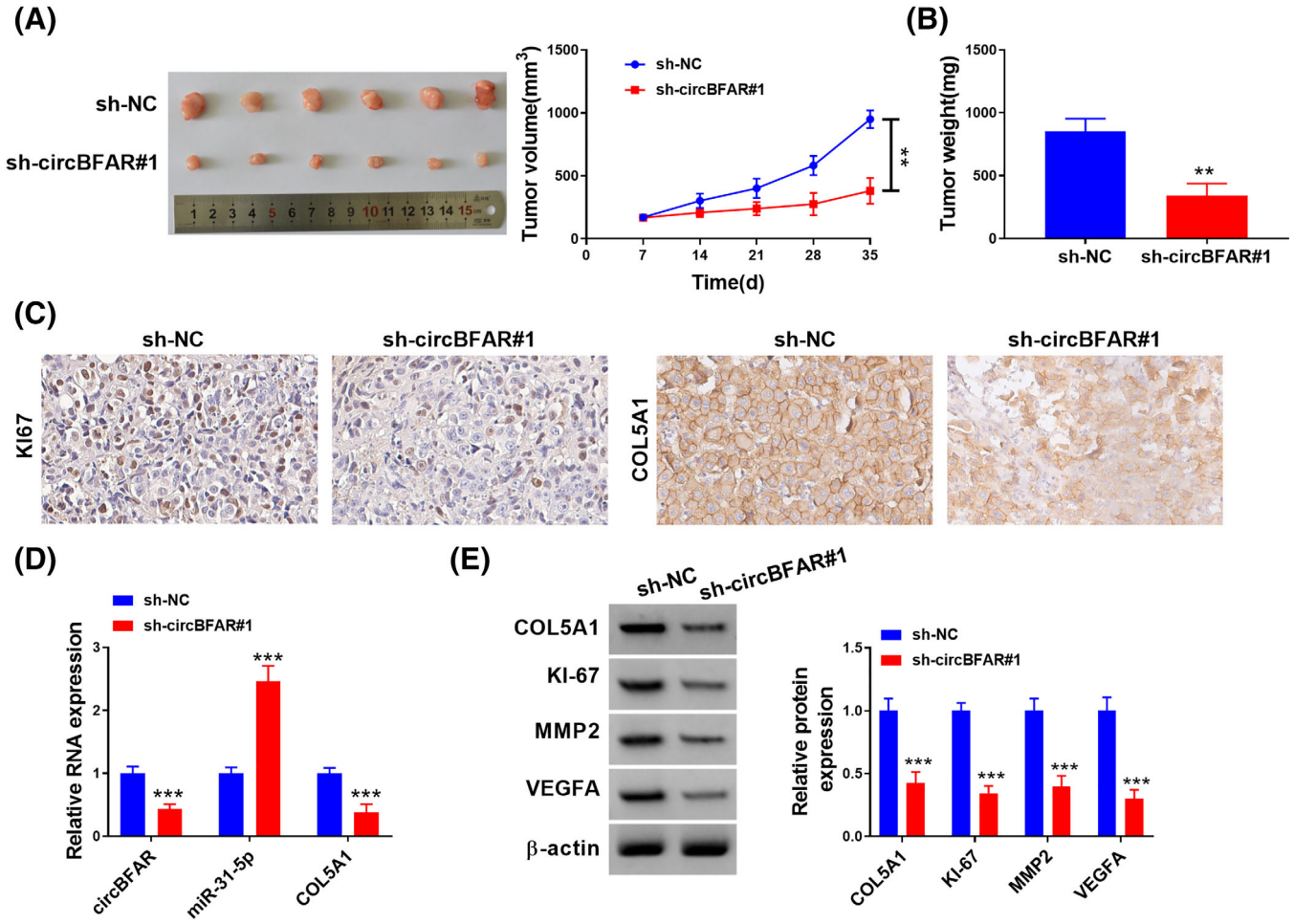

FIGURE 7 Silence of circBFAR could inhibit the tumor growth of laryngeal squamous cell cancer in vivo. (A) The tumor volume was measured every 7 days. (B) Tumor weight was detected in each group at the ending point. (C) The protein expression level of KI67 and collagen type V alpha 1 chain (COL5A1) in the sh-circBFAR#1 group was measured. (D) The expression of circBFAR, miR-31-5p, and COL5A1 was examined in each group by qRT-PCR. (E) The expression of COL5A1, KI-67, matrix metallopeptidase 2 (MMP2), and vascular endothelial growth factor A (VEGFA) in tissues was detected by western blot. *$p < .05$

miR-31-5p cotransfection group, while the luciferase activity in COL5A1-3′UTR-MUT and miR-31-5p cotransfection group did not change obviously (Figure 5D). And COL5A1 was negatively regulated by miR-31-5p in TU177 and AMC-HN-8 cells (Figure 5E,F). We also discovered that the expression of COL5A1 was blocked by sh-circBFAR#1 in TU177 and AMC-HN-8 cells, and the effect was abolished after anti-miR-31-5p cotransfection (Figure 5G). We found that COL5A1 was highly expressed in head and neck squamous cell carcinoma in the TCGA database (Figure 5H). And we discovered that COL5A1 was prominently elevated in LSCC tissues and cells (Figure 5I–K). In a word, COL5A1 was negatively regulated by miR-31-5p in LSCC cells.

3.6 | Overexpression of COL5A1 partially recuperated the inhibitory effects of miR-31-5p on LSCC cells

The expression of COL5A1 was abnormally reinforced in TU177 and AMC-HN-8 cells with COL5A1 transfection (Figure 6A). And the function rescue experiments uncovered that miR-31-5p inhibited cell viability and proliferation in TU177 and AMC-HN-8 cells, and COL5A1 cotransfection abated these effects (Figure 6B-C). And overexpression of miR-31-5p constrained cell migration and invasion, and the effects were ameliorated after COL5A1 was cotransfected (Figure 6D,E). The tube formation was inhibited by miR-31-5p, and this effect was weakened by COL5A1 overexpression (Figure 6F). The protein expression of KI-67, MMP2, and VEGFA in TU177 and AMC-HN-8 cells was suppressed by miR-31-5p, and COL5A1 cotransfection ameliorated these effects (Figure 6G). In brief, the inhibitory effects of miR-31-5p on LSCC cells were reverted by COL5A1 overexpression.

3.7 | Silencing of circBFAR inhibited the growth of LSCC in vivo

To confirm the role of circBFAR in vivo, tumor xenograft mice models were constructed. The results displayed that the volume and weight

of tumor tissues in the sh-circBFAR#1 group were effectively hampered compared with the sh-NC group (Figure 7A,B). And the data of immunohistochemistry speculated that the protein expression of KI67 and COL5A1 in the tissues of sh-circBFAR#1 group was robustly curbed (Figure 7C). The expression of circBFAR and COL5A1 in the sh-circBFAR#1 group was decreased, while miR-31-5p was increased in the sh-circBFAR#1 group when compared with the sh-NC group (Figure 7D). The results of western blot indicated that the protein expression of COL5A1, KI-67, MMP2, and VEGFA in the sh-circBFAR#1 group was impeded with respect to the sh-NC group (Figure 7E). In a word, circBFAR knockdown inhibited the growth of LSCC tumor in vivo.

4 | DISCUSSION

LSCC is the second most common malignancy of the head and neck, the prognosis is poor in advanced patients.[25] In this study, we clarified the mechanism of circBFAR in LSCC, which might provide a new target for the treatment and prognosis of LSCC.

A variety of circRNAs have been uncovered to be involved in the development of LSCC,[26–28] and we studied the function of circBFAR in LSCC. Guo et al.[29] found that circBFAR was upregulated as an oncogene in patients with pancreatic ductal adenocarcinoma (PDAC), which was pertinent to tumor node metastasis and poor prognosis of PDAC patients. We found that circBFAR was conspicuously expedited in LSCC tissues and cells, and was associated with advanced clinical stage and overall survival of LSCC patients. The data of function experiments exhibited that circBFAR knockdown markedly restrained cell viability, proliferation, migration, invasion, and tube formation in LSCC cells. And the protein expression of KI-67, MMP2 and VEGFA in LSCC cells was robustly suppressed by sh-circBFAR#1. At the same time, silence of circBFAR retarded tumor growth in vivo. In brief, the downregulation of circBFAR blocked the development and tumor growth of LSCC in vitro and in vivo.

It's reported that circRNAs, stable transcripts with a host of miRNA-binding sites, could act as sponges of miRNAs.[24,30] In this study, miR-31-5p was foretold to be the downstream gene of circBFAR though circinteractome, and the results of dual-luciferase reporter assay, RNA-pull down assay, and RIP assay indicated that circBFAR could sponge miR-31-5p in LSCC cells. MiR-31-5p was a subtype of miR-31, and our data manifested that miR-31-5p was evidently hindered in LSCC tissues and cells. It has been confirmed that miR-31 upregulation might hinder the growth and invasion of LSCC.[16] Similarly, our results proved that the inhibitory effects of circBFAR downregulation on viability, proliferation, migration, invasion, and angiogenesis in LSCC cells were overturned by anti-miR-31-5p. Consistently, decreased miR-31-5p reversed the suppression of circBFAR absence on the protein expression of KI-67, MMP2, and VEGFA in LSCC cells. In sum, circBFAR served as a sponge of miR-31-5p in LSCC cells, and anti-miR-31-5p cotransfection rescued the effects of sh-circBFAR#1 in LSCC cells.

COL5A1 was forecasted to be one of the target genes of miR-31-5p and was negatively regulated by miR-31-5p. We also suggested that COL5A1 was conspicuously augmented in LSCC. CircBFAR downregulation repressed COL5A1 expression in LSCC cells, and anti-miR-31-5p cotransfection ameliorated this effect. What's more, the prohibitive effects of miR-31-5p on cell viability and proliferation were neutralized by COL5A1 addition, and overexpression of miR-31-5p in TU177 and AMC-HN-8 cells hampered the cell migration, invasion and tube formation, and these effects were abated by COL5A1 overexpression. The protein expression of KI-67, MMP2, and VEGFA was blocked by miR-31-5p, and the inhibitory effects were recuperated after COL5A1 was cotransfected. In a word, circBFAR regulated the development of LSCC through miR-31-5p/COL5A1 axis.

5 | CONCLUSION

In this study, it was an unprecedented finding that circBFAR was enhanced in LSCC tissues and cells, and was concerned with the growth and prognosis of LSCC. The data of function rescue experiments disclosed that circBFAR regulated the progression of LSCC through the miR-31-5p/COL5A1 axis as an oncogene.

CONFLICT OF INTEREST

The author declares that there is no conflict of interest that could be perceived as prejudicing the impartiality of the research reported.

DATA AVAILABILITY STATEMENT

The analyzed data sets generated during this are available from the corresponding author on reasonable request.

ORCID

Di He https://orcid.org/0000-0002-8927-4555

REFERENCES

1. Almadori G, Bussu F, Cadoni G, Galli J, Paludetti G, Maurizi M. Molecular markers in laryngeal squamous cell carcinoma: towards an integrated clinicobiological approach. *Eur J Cancer*. 2005;41(5):683-693.
2. Rudolph E, Dyckhoff G, Becher H, Dietz A, Ramroth H. Effects of tumour stage, comorbidity and therapy on survival of laryngeal cancer patients: a systematic review and a meta-analysis. *Eur Arch Otorhinolaryngol*. 2011;268(2):165-179.
3. Kristensen LS, Andersen MS, Stagsted LVW, Ebbesen KK, Hansen TB, Kjems J. The biogenesis, biology and characterization of circular RNAs. *Nat Rev Genet*. 2019;20(11):675-691.
4. Patop IL, Wust S, Kadener S. Past, present, and future of circRNAs. *EMBO J*. 2019;38(16):e100836.
5. Fan D, Wang C, Wang D, Zhang N, Yi T. Circular RNA circ_0000039 enhances gastric cancer progression through miR-1292-5p/DEK axis. *Cancer Biomark*. 2021;30(2):167-177.
6. Lu C, Shi X, Wang AY, et al. RNA-Seq profiling of circular RNAs in human laryngeal squamous cell carcinomas. *Mol Cancer*. 2018;17(1):86.
7. Fan Y, Xia X, Zhu Y, et al. Circular RNA expression profile in laryngeal squamous cell carcinoma revealed by microarray. *Cell Physiol Biochem*. 2018;50(1):342-352.
8. Fu D, Huang Y, Gao M. Hsa_circ_0057481 promotes laryngeal cancer proliferation and migration by modulating the miR-200c/ZEB1 axis. *Int J Clin Exp Pathol*. 2019;12(11):4066-4076.

9. Bai Y, Hou J, Wang X, et al. Circ_0000218 plays a carcinogenic role in laryngeal cancer through regulating microRNA-139-3p/Smad3 axis. *Pathol Res Pract*. 2020;216(9):153103.
10. Wang Y, Cao B, Zhao R, Li H, Wei B, Dai G. Knockdown of circBFAR inhibits proliferation and glycolysis in gastric cancer by sponging miR-513a-3p/hexokinase 2 axis. *Biochem Biophys Res Commun*. 2021;560:80-86.
11. Li C, Guan X, Jing H, et al. Circular RNA circBFAR promotes glioblastoma progression by regulating a miR-548b/FoxM1 axis. *FASEB J*. 2022;36(3):e22183.
12. Lapa RML, Barros-Filho MC, Marchi FA, et al. Integrated miRNA and mRNA expression analysis uncovers drug targets in laryngeal squamous cell carcinoma patients. *Oral Oncol*. 2019;93:76-84.
13. Luo M, Sun G, Sun JW. MiR-196b affects the progression and prognosis of human LSCC through targeting PCDH-17. *Auris Nasus Larynx*. 2019;46(4):583-592.
14. Shuang Y, Li C, Zhou X, Huang YW, Zhang L. Expression of miR-195 in laryngeal squamous cell carcinoma and its effect on proliferation and apoptosis of Hep-2. *Eur Rev Med Pharmacol Sci*. 2017;21(14):3232-3238.
15. Shen X, Lei J, Du L. miR-31-5p may enhance the efficacy of chemotherapy with Taxol and cisplatin in TNBC. *Exp Ther Med*. 2020;19(1):375-383.
16. Yang S, Wang J, Ge W, Jiang Y. Long non-coding RNA LOC554202 promotes laryngeal squamous cell carcinoma progression through regulating miR-31. *J Cell Biochem*. 2018;119(8):6953-6960.
17. Huang GJ, Luo MS, Chen GP, Fu MY. MiRNA-mRNA crosstalk in laryngeal squamous cell carcinoma based on the TCGA database. *Eur Arch Otorhinolaryngol*. 2018;275(3):751-759.
18. Feng G, Ma HM, Huang HB, et al. Overexpression of COL5A1 promotes tumor progression and metastasis and correlates with poor survival of patients with clear cell renal cell carcinoma. *Cancer Manag Res*. 2019;11:1263-1274.
19. Liu W, Wei H, Gao Z, et al. COL5A1 may contribute the metastasis of lung adenocarcinoma. *Gene*. 2018;665:57-66.
20. Wu M, Sun Q, Mo CH, et al. Prospective molecular mechanism of COL5A1 in breast cancer based on a microarray, RNA sequencing and immunohistochemistry. *Oncol Rep*. 2019;42(1):151-175.
21. Wei Z, Chen L, Meng L. LncRNA HOTAIR promotes the growth and metastasis of gastric cancer by sponging miR-1277-5p and upregulating COL5A1. *Gastric Cancer*. 2020;23(6):1018-1032.
22. Zhang J, Zhang J, Wang F, et al. Overexpressed COL5A1 is correlated with tumor progression, paclitaxel resistance, and tumor-infiltrating immune cells in ovarian cancer. *J Cell Physiol*. 2021;236(10):6907-6919.
23. Han B, Chao J, Yao H. Circular RNA and its mechanisms in disease: from the bench to the clinic. *Pharmacol Ther*. 2018;187:31-44.
24. Panda AC. Circular RNAs act as miRNA sponges. *Adv Exp Med Biol*. 2018;1087:67-79.
25. Chu EA, Kim YJ. Laryngeal cancer: diagnosis and preoperative work-up. *Otolaryngol Clin North Am*. 2008;41(4):673-695.
26. Duan X, Shen N, Chen J, Wang J, Zhu Q, Zhai Z. Circular RNA MYLK serves as an oncogene to promote cancer progression via microRNA-195/cyclin D1 axis in laryngeal squamous cell carcinoma. *Biosci Rep*. 2019;39(9):BSR20190227.
27. Wu Y, Zhang Y, Zheng X, et al. Circular RNA circCORO1C promotes laryngeal squamous cell carcinoma progression by modulating the let-7c-5p/PBX3 axis. *Mol Cancer*. 2020;19(1):99.
28. Zhao J, Li XD, Wang M, Song LN, Zhao MJ. Circular RNA ABCB10 contributes to laryngeal squamous cell carcinoma (LSCC) progression by modulating the miR-588/CXCR4 axis. *Aging*. 2021;13(10):14078-14087.
29. Guo X, Zhou Q, Su D, et al. Circular RNA circBFAR promotes the progression of pancreatic ductal adenocarcinoma via the miR-34b-5p/MET/Akt axis. *Mol Cancer*. 2020;19(1):83.
30. Hansen TB, Jensen TI, Clausen BH, et al. Natural RNA circles function as efficient microRNA sponges. *Nature*. 2013;495(7441):384-388.

How to cite this article: Gong H, Wu W, Fang C, He D. CircBFAR correlates with poor prognosis and promotes laryngeal squamous cell cancer progression through miR-31-5p/COL5A1 axis. *Laryngoscope Investigative Otolaryngology*. 2022;7(6):1951-1962. doi:10.1002/lio2.966